Geometrical-Frustration-Induced (Semi)Metal-to-Insulator Transition

Satoshi Fujimoto

Department of Physics, Kyoto University, Kyoto 606-8502, Japan

(Received 24 July 2002; published 7 November 2002)

We study the low-energy properties of the geometrically frustrated Hubbard model on a three-dimensional pyrochlore lattice and a two-dimensional checkerboard lattice on the basis of the renormalization group method and mean field analysis. It is found that, in the half-filling case, a (semi)metal to insulator transition (MIT) occurs. Also, in the insulating phase, which has a spin gap, the spin rotational symmetry is not broken, while charge ordering exists. The results are applied to the description of the MIT observed in the pyrochlore system $Tl_2Ru_2O_7$.

DOI: 10.1103/PhysRevLett.89.226402 PACS numbers: 71.30.+h, 71.27.+a, 75.10.Lp

Recently, the role of geometrical frustration in both localized and itinerant electron systems has attracted renewed interest [1–8]. In localized systems, the possibility of an exotic phase such as a spin liquid without long-range magnetic order has been extensively investigated both experimentally [1,2,7,8] and theoretically [3–6]. In itinerant systems, the presence of charge degrees of freedom provides a route for the relaxation of magnetic frustration. However, when electron correlation is sufficiently strong, the magnetic frustration may still affect the low-energy properties significantly. For example, it has been found experimentally that some pyrochlore oxides, such as $Tl_2Ru_2O_7$ and $Cd_2Os_2O_7$, exhibit a (semi)metal to insulator transition (MIT) at finite critical temperatures [7,8]. Since such systems possess the fully frustrated lattice structure, referred to as a network of corner-sharing tetrahedra (that is, a pyrochlore lattice), the magnetic properties of the insulating phase are yet largely unexplained. Moreover, the mechanism of the MITs observed in these systems is still an open problem. Geometrical frustration may play an important role in the MITs. From this point of view, in the present paper, we study the interplay between electron correlation and geometrical frustration in the Hubbard model on a three-dimensional (3D) pyrochlore lattice and on a two-dimensional (2D) checkerboard lattice, the so-called 2D pyrochlore (Fig. 1). Although real pyrochlore oxides have electronic structure composed of t_{2g} orbitals, the present study on these simpler single-band models may provide important insight into the role of geometrical frustration in MIT. Furthermore, $Tl_2Ru_2O_7$ has, apart from the t_{2g} band, a nearly half-filled Tl s band, whose important features are described by the 3D pyrochlore Hubbard model [9]. We believe that this model may provide a useful understanding of the MIT undergone in this material.

The noninteracting energy bands of these two Hubbard models have a common interesting feature: They consist of a flat band (or two degenerate flat bands) on the upper band edge and a dispersive band that is tangent to the flat band (or flat bands) at the Γ point [10]. According to graph theory, this band structure stems from the geometrical frustration inherent in the pyrochlore lattice. In the half-filling case, $n = 1$, on which we concentrate henceforth, the dispersive band is fully occupied, and the flat band(s) is empty. In the noninteracting half-filling case, the system is in a semimetal state, since the Fermi velocity is vanishing, though there is no excitation gap. We study how this state is affected by electron correlation.

Diagonalizing the kinetic term, we write the Hamiltonian as

$$H = \sum_{\mu=1}^{m} \sum_{k\sigma} E_{k\mu} a^{\dagger}_{k\mu\sigma} a_{k\mu\sigma} + \frac{U}{N} \sum_{k,k',q} \sum_{\alpha\beta\gamma\delta} \Gamma^{0}_{\alpha\beta\gamma\delta}(k-q, k'+q; k', k) a^{\dagger}_{k-q\alpha\uparrow} a^{\dagger}_{k'+q\beta\downarrow} a_{k'\gamma\downarrow} a_{k\delta\uparrow},$$

$$\Gamma^{0}_{\alpha\beta\gamma\delta}(k_1, k_2; k_3, k_4) = \sum_{\nu=1}^{m} s_{\nu\alpha}(\boldsymbol{k}_1) s_{\nu\beta}(\boldsymbol{k}_2) s_{\nu\gamma}(\boldsymbol{k}_3) s_{\nu\delta}(\boldsymbol{k}_4), \tag{1}$$

where $m = 2$ in the 2D case, and $m = 4$ in the 3D case. In the 2D case, $E_{k1} = 2$, $E_{k2} = 4\cos k_x \cos k_y - 2$, $s_{11}(\boldsymbol{k}) = s_{22}(\boldsymbol{k}) = \sin[(k_x + k_y)/2]/\sqrt{1 - \cos k_x \cos k_y}$, and $s_{21}(\boldsymbol{k}) = -s_{12}(\boldsymbol{k}) = \sin[(k_x - k_y)/2]/\sqrt{1 - \cos k_x \cos k_y}$. In the 3D case, $E_{k1} = E_{k2} = 2$, $E_{k3} = -2 + 2\sqrt{1 + t_k}$, and $E_{k4} = -2 - 2\sqrt{1 + t_k}$, with $t_k = \cos(2k_x)\cos(2k_y) + \cos(2k_y)\cos(2k_z) + \cos(2k_z)\cos(2k_x)$. The form of $s_{\mu\nu}(\boldsymbol{k})$ in the 3D case is given in Ref. [6]. The annihilation operator of electrons at the μth site in a unit cell is given by $c_{k\mu\sigma} = \sum_{\nu=1}^{m} s_{\mu\nu}(\boldsymbol{k}) a_{k\nu\sigma}$.

As shown in Ref. [6], the perturbative calculation in U for the above Hamiltonian suffers from divergences at third and higher order, due to the presence of the flat band(s). To treat the divergences in a controlled manner, we apply the renormalization group (RG) method. In previous studies of electron systems [11], a momentum

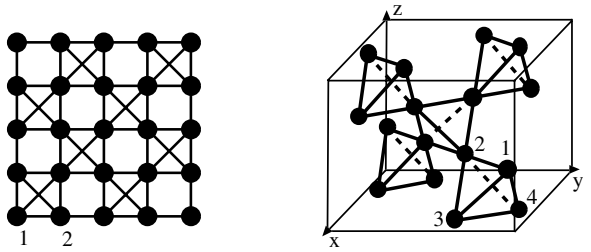

2D Checkerboard Pyrochlore 3D Pyrochlore Lattice

FIG. 1. 2D and 3D pyrochlore lattices.

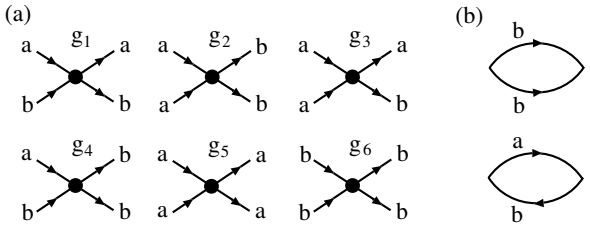

FIG. 2. (a) The six species of four-point vertices. Here "a" and "b" indicate the dispersive band and the flat band, respectively. (b) The leading singular bubble diagrams.

cutoff that separates the neighborhood of the Fermi surface from the higher momentum part is introduced. However, in the presence of the flat band(s), this procedure is not applicable. To overcome this problem, we introduce the infrared energy cutoff Λ in the following manner: $\psi_{\mu\sigma}(k, \varepsilon_n) = \psi^{>}_{\mu\sigma}(k, \varepsilon_n)\Theta(|\varepsilon_n| - \Lambda) + \psi^{<}_{\mu\sigma}(k, \varepsilon_n)\Theta(\Lambda - |\varepsilon_n|)$. Here, $\psi_{\mu\sigma}(k, \varepsilon)$ is the Grassmann field corresponding to $a_{k\mu\sigma}$.

Using a standard method, we can obtain the RG equations of the single-particle self-energy, $\Sigma_{\mu\nu}(k)$, and the four-point vertex functions, $\Gamma_{\alpha\beta\gamma\delta}(k_1, k_2; k_3, k_4)$, up to the one-loop order. In our systems, there are six species of four-point vertices, as shown in Fig. 2(a), apart from the spin degrees of freedom and the twofold degeneracy of the flat bands in the 3D case. We assume that the momentum dependences of the four-point vertex functions are given mainly by $\Gamma^0(k_1, k_2; k_3, k_4)$ in the renormalization processes. This is made explicitly by replacing $\Gamma_{abab}(k_1, k_2; k_3, k_4)$ with $g_1\Gamma^0_{abab}(k_1, k_2; k_3, k_4)$, $\Gamma_{bbba}(k_1, k_2; k_3, k_4)$ with $g_4\Gamma^0_{bbba}(k_1, k_2; k_3, k_4)$, etc. This approximation is fairly good, because in the vicinity of the Γ point, where the most important scattering processes occur, the band structure is almost isotropic. Because the flat bands are empty and the dispersive band is fully occupied, the particle-particle processes between the flat bands and the particle-hole processes between the flat bands and the dispersive band give the leading singular contributions [see Fig. 2(b)]. We take into account these contributions in the derivation of the RG equations. We found from the analysis of the RG equations that, among the six running couplings, g_2, g_3, and g_5 are irrelevant in the low-energy limit. The RG equations for the other couplings, g_1, g_4, and g_6, are written

$$\frac{dg_{1s}}{dl} = -\frac{ag_{4s}^2 e^l}{\Lambda_0} + \frac{b(\Lambda_0 e^{-l})^\eta}{4}(g_{1s}^2 + 6g_{1s}g_{1t} - 3g_{1t}^2), \tag{2}$$

$$\frac{dg_{1t}}{dl} = \frac{b(\Lambda_0 e^{-l})^\eta}{4}(g_{1s}^2 - 2g_{1s}g_{1t} + 5g_{1t}^2), \tag{3}$$

$$\frac{dg_{4s}}{dl} = -\frac{ag_{4s}g_{6s}}{\Lambda_0} e^l + \frac{b(\Lambda_0 e^{-l})^\eta}{4}(g_{1s}g_{4s} + 3g_{4s}g_{1t}), \tag{4}$$

$$\frac{dg_{6s}}{dl} = -\frac{ag_{6s}^2}{\Lambda_0} e^l, \tag{5}$$

where $\eta = (d-2)/2$, $l = \ln(\Lambda_0/\Lambda)$, with Λ_0 the bandwidth, and d is the spatial dimension. The couplings g_{is} and g_{it} denote the spin singlet and triplet parts, respectively. In the 2D case, $a = \sum_k [s_{11}^4(k) - s_{11}^2(k)s_{12}^2(k)]/2$, $b = 1/(32t)$, and in the 3D case, $a = \sum_k \{[s_{11}^2(k) + s_{12}^2(k)]^2 - [s_{11}(k)s_{21}(k) + s_{12}(k)s_{22}(k)]^2\}/2$, and $b \approx 0.0775/t^{3/2}$. In the derivation of these equations for the 3D case, we have used the fact that, in the vicinity of the Γ point, the two degenerate flat bands do not mix with each other in scattering processes. Thus, in this case the twofold degeneracy just gives an overall factor of 2.

2D checkerboard pyrochlore.—We first consider the 2D case, whose theoretical treatment is simpler. We solved the RG equations (2)–(5) numerically for a particular set of parameter values, and obtained the RG flow shown in Fig. 3(a). We found that, for any small value of U/t, g_{1t} flows into the strong-coupling regime. This indicates some instability in this channel. Although g_{1s} also scales into the strong-coupling regime, it is subdominant compared to g_{1t}. We also show in Fig. 3(a) the RG flows of the couplings $3g_{1t} - g_{1s}$ and $g_{1s} + g_{1t}$, which are related to the charge and spin susceptibilities, respectively. We see that some instability appears in the charge degrees of freedom. To elucidate the nature of this instability, we write the RG equations for the single-particle self-energy in the following form:

$$\frac{d(\Sigma^\Lambda_{12\uparrow\uparrow} + \Sigma^\Lambda_{12\downarrow\downarrow})}{dl} = 2b(3g_{1t} - g_{1s})(\Sigma^\Lambda_{12\uparrow\uparrow} + \Sigma^\Lambda_{12\downarrow\downarrow}), \tag{6}$$

$$\frac{d(\Sigma^\Lambda_{12\uparrow\uparrow} - \Sigma^\Lambda_{12\downarrow\downarrow})}{dl} = 2b(g_{1s} + g_{1t})(\Sigma^\Lambda_{12\uparrow\uparrow} - \Sigma^\Lambda_{12\downarrow\downarrow}), \tag{7}$$

$$\frac{d\Sigma^\Lambda_{12\uparrow\downarrow}}{dl} = 2b(g_{1s} + g_{1t})\Sigma^\Lambda_{12\uparrow\downarrow}. \tag{8}$$

In the derivation of these equations, we have ignored the diagonal self-energy, which are not important in the following argument, and expanded the RG equations up to the first order in Σ^Λ_{12}. Because the strongest divergence of the four-point vertex appears in $3g_{1t} - g_{1s}$ [see Fig. 3(a)], the off-diagonal self-energy $\sum_\sigma \Sigma_{12\sigma\sigma}$

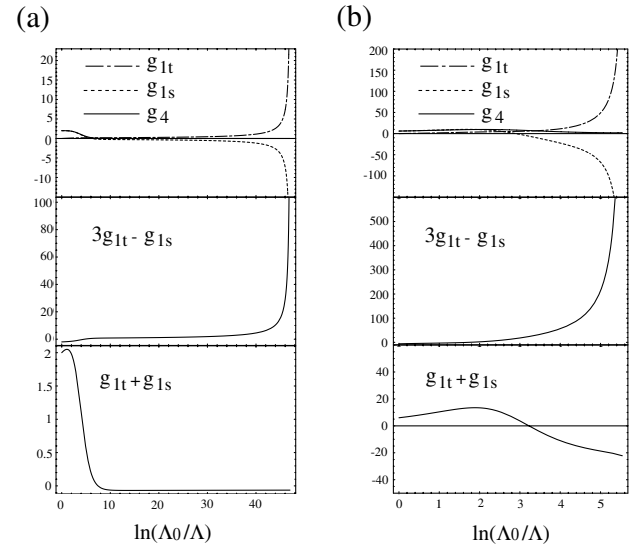

FIG. 3. (a) The RG flow of the running couplings in the 2D case with $U/8t = 0.25$. (b) The RG flow in the 3D case with $U/8t = 0.75$.

becomes nonzero at some critical $\Lambda = \Lambda_c$. This is easily seen by solving (6), which gives $\sum_\sigma \Sigma^{\Lambda}_{12\sigma\sigma} = \sum_\sigma \Sigma^{\Lambda_0}_{12\sigma\sigma} \exp[2b \int_0^l dl'(3g_{1t} - g_{1s})]$. Note that $\Sigma^{\Lambda_0}_{12\sigma\sigma}$ is vanishing in the vicinity of the Γ point, because of the momentum dependence of $s_{\mu\nu}(k)$. Thus, for $\Lambda = \Lambda_c$ at which value $3g_{1t} - g_{1s}$ is divergent, $\sum_\sigma \Sigma^{\Lambda_c}_{12\sigma\sigma}$ becomes nonzero.

The above RG analysis implies the existence of a mean field solution for which the order parameter is given by $\Delta_k \equiv \sum_\sigma \Sigma_{12\sigma\sigma}(k) \sim \sum_{\sigma=\uparrow\downarrow} \langle a^\dagger_{k1\sigma} a_{k2\sigma} \rangle$. This state is characterized by electron-hole pairing with parallel spins, which leads to the formation of both spin and charge gaps preserving the spin rotational symmetry. According to the numerical analysis of the RG equations (2)–(5), g_{4s} is mainly renormalized by the first term of the right-hand side of (4). Then, the renormalized coupling g_{4s} is approximately given by RPA-like expressions. As a result, we obtain the self-consistent gap equation for Δ_k expressed diagrammatically in Fig. 4. The transition temperature is determined from the linearized gap equation,

$$\Delta_k = \sum_{q,k'} \Pi(k, q-k) G_{11}(q-k) G_{22}(q-k) \times \Pi(k', q-k) G_{11}(k') G_{22}(k') \Delta_{k'}, \quad (9)$$

where $G_{\mu\mu}(k) = 1/(\varepsilon_n - E_{k\mu})$, $k = (i\varepsilon, \boldsymbol{k})$, and $\Pi(k, k') = \sum_{\nu=\pm} \nu U t^\nu(\boldsymbol{k}, \boldsymbol{k}')/[1 - c_\nu D(k + k')]$, $t^\pm[\boldsymbol{k}, \boldsymbol{k}'] = (s_{11}(\boldsymbol{k}) s_{12}(\boldsymbol{k}') \pm s_{12}(\boldsymbol{k}) s_{11}(\boldsymbol{k}'))^2/2$ with

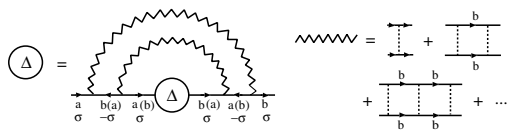

FIG. 4. Diagrams for the linearized gap equations.

$D(q) = -TU \sum_{n,k} G_{11}(k) G_{11}(q-k)$, $c_+ = 2a$, and $c_- = \sum_k s^2_{11}$. Here, we have ignored the diagonal self-energy. Equation (9) implies that the gap function can be written $\Delta_k = s_{11}(k) s_{12}(k) \Delta_0$, where Δ_0 is a constant. From (9), we have $\Delta_0 = \Delta_0 (U^2/16t)[\ln(8t/U) - b_0] \ln(8t/T_c)$, where $b_0 = 0.322$. For $U < U_c \sim 0.725 \times 8t$, a state with nonzero Δ_0 is realized. We have also applied the Ginzburg-Landau analysis to this mean field solution and found that, in the 2D case, the transition temperature vanishes in accordance with the Mermin-Wagner-Coleman theorem. Nevertheless, the above analysis demonstrates that, in the ground state at zero temperature, the gap Δ_k is nonzero, and the system is in an insulating state.

We now further investigate the properties of the insulating phase. In this phase, because the order parameter does not break the spin rotational symmetry, there is no long-range magnetic order. However, a spin gap exists. The spin-spin correlation function obtained from the above mean field solution is $\mathrm{Im}\,\chi_s(q, \omega)/\omega \sim \langle 1/[2T \cosh^2(\Delta_k/2T)] \rangle_{k\sim 0}$ for $\omega \to 0$. Here, $\langle \cdots \rangle_{k\sim 0}$ is the angular average near $k = 0$. This spin gap behavior can be observed using NMR measurements.

Another important property of the insulating phase involves the charge degrees of freedom. The formation of the gap Δ_k gives rise to a difference between the charge densities at sites 1 and 2 in a unit cell given by $\rho_1 - \rho_2 \sim \Delta_0/t$, up to a constant factor. Thus, charge ordering (CO) with a charge density displacement proportional to the gap characterizes this insulating state [see Fig. 5(a)]. This noteworthy result can be understood as follows. In our system, three electrons occupying nearest neighbor sites cost energy loss caused by magnetic frustration. Conversely, magnetic frustration induces an effective finite-range repulsion between electrons at nearest neighbor sites. If this finite-range repulsion is sufficiently strong to overcome the on-site Coulomb interaction U, the CO state will be stabilized. This is possible if U is not so large. As U increases, a transition to a conventional Mott insulator with no charge ordering should occur. This transition cannot be described within our weak-coupling analysis.

3D pyrochlore.—The above analysis can be straightforwardly generalized to the case of a 3D pyrochlore lattice. We obtain the RG flow numerically from (2)–(5) for $d = 3$. Here, in contrast to the 2D case, for sufficiently small U all couplings are irrelevant, and thus the semimetal state is stable. However, for values of U larger than a certain critical value but still smaller than the

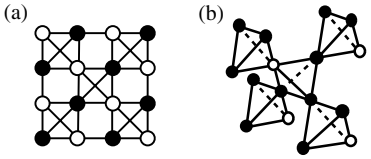

FIG. 5. (a) The CO pattern in the 2D case. (b) The CO pattern in the 3D case.

bandwidth, RG flow similar to that in the 2D case is obtained, as shown in Fig. 3(b). The coupling $3g_{1t} - g_{1s}$, which is related to the charge degrees of freedom, scales into the strong-coupling regime. This RG flow implies that, as in the 2D case, a particle-hole pairing state with order parameters $\Delta_k^{(13)} = \sum_\sigma \langle a_{k1\sigma}^\dagger a_{k3\sigma} \rangle$ and $\Delta_k^{(23)} = \sum_\sigma \langle a_{k2\sigma}^\dagger a_{k3\sigma} \rangle$ is realized. Although the value of U used here is relatively large, we expect that the one-loop RG calculation still gives qualitatively correct results, as long as U is smaller than the bandwidth. To examine the validity of the one-loop calculation, we explore the self-consistent mean field solution. The self-consistent gap equations for the 3D case are also given by the diagram shown in Fig. 4, from which we find that the gap functions are given by $\Delta_k^{(13)} = \sum_{\nu=1}^4 s_{\nu 1}(k) s_{\nu 3}(k) \Delta_\nu^{(13)}$, $\Delta_k^{(23)} = \sum_{\nu=1}^4 s_{\nu 2}(k) s_{\nu 3}(k) \Delta_\nu^{(23)}$. Using the symmetry properties of $s_{\mu\nu}(k)$ in momentum space, we can show without solving the gap equations that $\Delta_\nu^{(13)} = 0$, and $\Delta_1^{(23)} = \Delta_2^{(23)} = \Delta_3^{(23)}$. Thus, from the orthogonal relations among the $s_{\mu\nu}(k)$, we have $\Delta_k^{(23)} = s_{42}(k) s_{43}(k) [\Delta_4^{(23)} - \Delta_1^{(23)}]$. The quantity $\Delta_4^{(23)} - \Delta_1^{(23)}$ is determined from the gap equation. According to the RG analysis, the transition occurs only for sufficiently large U. Therefore, to determine the transition temperature and the gap function correctly, we need to take into account the self-energy corrections, i.e., pair breaking effect. This calculation is rather involved, and we have not yet carried it out. However, we see from the RG flow that at the critical temperature $T_c \sim \Lambda_0 e^{-l_c} = 8t \times 0.004$, a transition from a semimetal to an insulator occurs. In the resulting insulating state, the threefold degeneracy at the Γ point in the semimetal state is lifted completely, and a spin gap as well as a charge gap exists.

As in the 2D case, we examine now the possibility of a CO state in the 3D system. In this case, there are four sites in a unit cell. The appearance of a gap causes a charge density displacement on each site given by $\delta\rho_\nu = 2 \sum_k s_{\nu 2}(k) s_{\nu 3}(k) \Delta_k^{(23)}$ for $\nu = 1, 2, 3$. Using the symmetry properties of $s_{\mu\nu}(k)$, we find $\delta\rho_1 = \delta\rho_2 = \delta\rho_3 \neq 0$ and $\delta\rho_4 = -3\delta\rho_1$. It is thus found that CO with the pattern displayed in Fig. 5(b) occurs in the insulating phase. Interestingly, a similar CO pattern is observed in the spinel system AlV_2O_4 which possesses a V-site corner-sharing tetrahedron network [12].

We now apply the results obtained above to the description of the MIT observed in $Tl_2Ru_2O_7$. The band calculation gives the bandwidth of this system $8t \sim 2$ eV [9]. Experimental data on the size of U do not exists. However, typically, the value of U for transition metal oxides is $\sim$2 eV. This gives us reason to believe that the analysis given in this paper, which suggests that the MIT occurs for large $U \sim 8t$, can be applied to the description of the $Tl_2Ru_2O_7$ system. The transition temperature estimated from the RG analysis is $T_c \sim 96$ K, which is almost comparable with the experimental values $100 \sim 120$ K [7]. A recent NMR measurement has revealed the presence of a spin gap in the insulating state, which is consistent with our results [13]. The possible existence of a CO state and large enhancement of charge fluctuations above T_c predicted in our theory have not yet been investigated experimentally. The experimental determination of whether a CO state exists for $Tl_2Ru_2O_7$ is a crucial test of this theory. When there exists coupling to a lattice, CO should accompany lattice distortion. It has been found experimentally that, in $Tl_2Ru_2O_7$, the lattice structure changes from cubic to orthorhombic at the MIT point. This observation seems to suggest the presence of large charge fluctuations in this system.

In conclusion, the 2D and 3D pyrochlore Hubbard models at the half filling show the transition from semimetal to spin-gapped insulator. In the insulating state, charge ordering occurs so as to relax geometrical frustration.

The author is grateful to K. Yamada and H. Tsunetsugu for comments and discussions. This work was supported by a Grant-in-Aid from the Ministry of Education, Science, and Culture, Japan.

[1] A. P. Ramirez, Annu. Rev. Mater. Sci. **24**, 453 (1994).
[2] B. D. Gaulin *et al.*, Phys. Rev. Lett. **69**, 3244 (1992); M. J. Harris *et al.*, Phys. Rev. Lett. **73**, 189 (1994); D. Yanagishima and Y. Maeno, J. Phys. Soc. Jpn. **70**, 2880 (2001); Y. J. Uemura *et al.*, Phys. Rev. Lett. **73**, 3306 (1994); R. Coldea *et al.*, Phys. Rev. Lett. **86**, 1335 (2001).
[3] R. Moessner and J. T. Chalker, Phys. Rev. Lett. **80**, 2929 (1998); J. N. Reimers, Phys. Rev. B **45**, 7287 (1992); B. Canals and C. Lacroix, Phys. Rev. Lett. **80**, 2933 (1998); A. B. Harris, A. J. Berlinsky, and C. Bruder, J. Appl. Phys. **69**, 5200 (1991); M. Isoda and S. Mori, J. Phys. Soc. Jpn. **67**, 4022 (1998); Y. Yamashita and K. Ueda, Phys. Rev. Lett. **85**, 4960 (2000); A. Koga and N. Kawakami, Phys. Rev. B **63**, 144432 (2001); H. Tsunetsugu, J. Phys. Soc. Jpn. **70**, 640 (2001).
[4] S. E. Palmer and J. T. Chalker, Phys. Rev. B **64**, 094412 (2001); E. H. Lieb and P. Schupp, Phys. Rev. Lett. **83**, 5362 (1999); O. A. Starykh, R. R. P. Singh, and G. C. Levine, Phys. Rev. Lett. **88**, 167203 (2002); E. Berg, E. Altman, and A. Auerbach, cond-mat/0206384.
[5] J. T. Chalker, P. C. W. Holdsworth, and E. F. Shender, Phys. Rev. Lett. **68**, 855 (1992); I. Ritchey, P. Chandra, and P. Coleman, Phys. Rev. B **47**, 15 342 (1993); P. Lecheminant *et al.*, Phys. Rev. B **56**, 2521 (1997).
[6] S. Fujimoto, Phys. Rev. B **64**, 085102 (2001); M. Isoda and S. Mori, J. Phys. Soc. Jpn. **69**, 1509 (2000).
[7] T. Takeda *et al.*, J. Solid State Chem. **140**, 182 (1998).
[8] D. Mandrus *et al.*, Phys. Rev. B **63**, 195104 (2001).
[9] F. Ishii and T. Oguchi, J. Phys. Soc. Jpn. **69**, 526 (2000).
[10] A. Mielke, J. Phys. A **24**, L73 (1991).
[11] R. Shankar, Rev. Mod. Phys. **66**, 129 (1994); C. Halboth and W. Metzner, Phys. Rev. B **61**, 7364 (2000); D. Zanchi and H. J. Schulz, Phys. Rev. B **61**, 13609 (2000); M. Salmhofer, *Renormalization* (Springer-Verlag, Berlin, 1998).
[12] K. Matsuno *et al.*, J. Phys. Soc. Jpn. **70**, 1456 (2001).
[13] H. Sakai *et al.*, J. Phys. Soc. Jpn. **71**, 422 (2002).